Effects of high-pressure treatment on the muscle structure of salmon (Salmo salar)

Camille Renaud, Marie de Lamballerie, Claire Guyon, Thierry Astruc, Annie Venien, Laurence Pottier

Effects of high-pressure treatment on the muscle structure of salmon (*Salmo salar*)

Camille RENAUD[1], Marie de LAMBALLERIE[1 *], Claire GUYON[1], Thierry ASTRUC[2], Annie VENIEN[2], Laurence POTTIER[1]

[1] UMR CNRS 6144 GEPEA, CS 82225, ONIRIS, Food Process Engineering, 44322 Nantes Cedex 3, France

[2] UR370 QuaPA, INRAe Clermont-Ferrand-Theix, F-63122 St Genès Champanelle, France

* Corresponding author. Phone number: +33251785454

E-mail address: marie.de-lamballerie@oniris-nantes.fr

Abstract

High pressure (HP) is a non-thermal treatment that is generally used to reduce the microbiological contamination of food products, such as Atlantic salmon (*Salmo salar*). However, HP is known to alter the stability of proteins and can therefore affect the quality of salmon flesh. In this study, the effects of HP treatment for 5 min at 200, 400 and 600 MPa on the structure of Atlantic salmon were investigated. Transversal histological sections revealed a decrease in the fibre size from 200 MPa associated with an expansion of the extracellular spaces. Connective tissue was found to be modified from 400 MPa, resulting in an increase in its surface area. Fourier transform infrared (FT-IR) microspectroscopy revealed a reduction in the α-helix content and an increase in the aggregated β-sheet structure content with increasing pressure, reflecting a change in the secondary structure of proteins from 200 MPa.

Keywords

High pressure, Salmon, Histology, Infrared microspectroscopy, Protein secondary structure, Muscle structure

1. Introduction

Atlantic salmon (*Salmo salar*) is the third most consumed fish in the European Union, with an apparent consumption per capita in 2018 of 2.24 kg live weight equivalent (Directorate-General for Maritime Affairs and Fisheries (European Commission), 2020). However, due to microbial, chemical and enzymatic activity, salmon is a highly perishable product with a shelf life of approximately ten days on ice (Fogarty et al., 2019). Among the numerous technologies that are being investigated to increase this shelf life, de Alba et al. (2019) and Park et al. (2015) have shown a significant effect of high pressure (HP) on microbial reduction. High-pressure treatments have been used since 1990 in Japan to process jams, jellies and sauces and are currently used for processing vegetables, meat and fish products, as well as juices and beverages (Oliveira et al., 2017). This technology represents a particularly interesting preservation technique because it tackles numerous issues of the food industry related to consumer expectations: it does not require the use of food additives to improve the product shelf life, it is more energy efficient than traditional technologies such as cooking (Truong et al., 2015) and it preserves fish nutrients, such as unsaturated fatty acids (Yagiz et al., 2009).

Nonetheless, this technology leads to modifications of food biopolymers, especially proteins, as a result of the thermodynamic effects of pressure. Indeed, according to the Le Chatelier principle, the application of HP favours changes causing a decrease in volume (Mozhaev et al., 1994). Consequently, phenomena such as disruption of hydrophobic and electrostatic interactions are promoted by HP, leading to changes in quaternary, tertiary and secondary structures. Covalent bonds, hydrogen bonds and disulphide bridges, on the other hand, have low compressibility and are expected to be resistant to pressure

(Aubourg, 2018; Knorr et al., 2006; Mozhaev et al., 1994; Oliveira et al., 2017).

Fish muscles are composed of approximately 20% proteins in total and are therefore particularly sensitive to HP. Fish meat consists mainly of myofibrillar proteins, which are responsible for muscle contraction; sarcoplasmic proteins, which are water soluble; and proteins from connective tissue such as collagen, which are insoluble extracellular proteins.

HP has been proven interesting to improve the quality of fish by reducing its susceptibility to oxidation (Yagiz et al., 2009) and by enhancing its sensory attributes such as taste, odour and texture (Truong et al., 2015). Moreover, HP has been used to ameliorate the freezing and thawing of different fish species, as it increases the kinetics of ice-water transitions, thus avoiding the formation of large ice crystals (Aubourg, 2018). The protein modifications caused by the pressure have also been used to improve the quality of fish gels (Truong et al., 2017; Uresti et al., 2004). However, several studies have shown unwanted effects of HP on the quality of fish fillets, such as an increased hardness and a change in colour with increased lightness after treatment at 150 MPa (Arnaud et al., 2018; Aubourg et al., 2013), giving the product a cooked appearance.-Even though the effects of HP on the sensory attributes of salmon have been widely described, the molecular mechanisms causing these modifications are still unclear. *In situ* approaches are therefore a powerful tool, as they allow precise analysis of the microscopic and biochemical alterations induced by treatment of the product while taking into account the complexity and high level of organization of the biological structures. The knowledge of the effects of HP on a microscopic and molecular scale should therefore help understanding the changes of fish quality and determine the ideal parameters of treatment to minimize the undesirable impacts of HP.

The purpose of this study was to investigate *in situ* the effects of a high-pressure treatment on both the microstructure and secondary structure of salmon muscle proteins.

2. Materials & Methods

2.1. Biological material

Twelve whole salmons (*Salmo salar*, farmed in Scotland) were purchased from a local supplier (Jean LEBEAUPIN, Nantes, France) one day after the harvesting date. The fish weighed 2.5 to 3 kg and were of “Label Rouge” quality, which is an official French label guaranteeing strict farming conditions and final product quality such as a lipid rate between 10 and 16%.

The collagen content in the muscle of the salmons, which was evaluated by an external laboratory (Inovalys, Nantes, France) and calculated as [(L)-hydroxyproline content x 8], was equal to 0.3 %. From each fish, a slice approximately 5 cm wide was excised and cut into four 40 g parts (see the supplementary material), which were each vacuum packed (98% vacuum) in individual polyamide/polyethylene bags (La Bovida, Paris, France) and kept on ice before processing. The remaining parts of the fish were stored at -20°C until further biochemical analysis.

2.2. Reagents and chemicals

For the HES staining, the following chemicals and reagents were used: Harris Haematoxylin (Harris Hematoxylin Surgipath, Leica biosystem, Buffalo Grove, IL, USA), Eosin 0.5% (eosin Y 0.5% w/v aqueous solution, Sigma Aldrich, St Louis, MO, USA), Powdered saffron (Technical, VWR International, Radnor, PA, USA), Methylcyclohexane (for synthesis, Merck, Darmstadt, Germany), Eukitt (Eukitt® Quick-hardening mounting medium, Sigma Aldrich, St Louis, MO, USA) and Ethanol (99%, Carlo Erba Reagents, Val de Reuil, France).

For the Picrosirius red staining, the following chemicals and reagents were used: Acetone

(99%, Sigma Aldrich, St Louis, MO, USA), Picro-Sirius red (Sirius red F3B, Gurr BDH laboratory Supplies, Poole, England), Hydrochloric acid 0.01M (37%, VWR International, Radnor, PA, USA), Ethanol (99%, Carlo Erba Reagents, Val de Reuil, France) and Methycyclohexane (for synthesis, Merck, Darmstadt, Germany). A Picro-formalin solution was prepared with ethanol 95% and formaldehyde (37 %, Sigma Aldrich, St Louis, MO, USA) (180/25 v/v) and picric acid to saturation (Powdered, Sigma Aldrich, St Louis, MO, USA).

2.3 High-pressure processing

The packed samples (approximately 40 g each) were inserted in the stainless steel chamber of a custom-made high-pressure device (NOVA SWISS, Cesson, France). The chamber, equipped with a water jacket and a temperature regulator device, was filled with water at 20°C and pressure was generated by addition of water in the chamber using a hydrostatic pump. For each fish, the four pieces were processed with a balanced experimental design for 5 min at 200 MPa, 400 MPa, 600 MPa or unpressurized (control), meaning that for each level of pressure, different locations of the salmon were used. These pressure rates were chosen in order to investigate the process effect up to 600 MPa which is generally the maximum HP used in industry and was the maximum limit of the equipment. The compression rate was 3 MPa/s, and the depression rates were 4 MPa/s, 8 MPa/s and 10 MPa/s respectively. During the pressurization process, the maximal temperatures reached were 24.7°C, 29.4°C and 33.6°C for the samples pressurized at 200, 400 and 600 MPa, respectively. The samples were kept on ice as soon as the treatment ended and until histological sampling.

2.4. Microstructure

2.4.1. Histochemical analysis

A 10 mm wide cube was cut from each sample to identify the muscle fibre direction. The cubes were plunged and stirred for 30 seconds in 2-methyl-butane (-160°C) cooled with liquid nitrogen (-196°C). The cryofixed samples were then kept at -80°C until analysis. A cryomicrotome (Leica CM 1950, Leica Biosystems, Nussloch, Germany) was used to cut 10 µm slices from each cube, transversally to the muscle fibre direction. The sections were mounted on SuperFrost microscope slides, air-dried (20°C) and stained with haematoxylin-eosin-saffron (HES) to contrast the tissue and visualize the general structure and with picrosirius red to reveal connective tissue. The stained sections were mounted with synthetic resin (Eukitt, Kindler GmbH & Co, Freiburg, Germany) and protected by covering with a glass coverslip. Images were acquired using an Olympus BX 61 microscope coupled with a high-resolution digital camera (Olympus DP 71) and Olympus Cell Sens software (Olympus France SAS, Rungis, France).

For each sample, at least ten images of x100-magnified HES staining and picrosirius staining were captured.

2.4.2. Image analysis

For each of the four conditions, ten images of HES staining and picrosirius staining were analysed using open-source ImageJ software (https://imagej.nih.gov/ij/). Approximately 50 muscle fibres were counted per optical field, which means that approximately 500 fibres per sample were analysed. For each picture, the software was used to calculate both the average size of the fibres and the percentage of surface occupied by the fibres, the connective tissue and the extracellular spaces (ECSs), per optical field.

2.5. Infrared spectroscopy data acquisition

Histological cross-sections (6 µm thick) were obtained from the cryofixed muscle sample, collected on a BaF_2 window with IR spectroscopy compatibility (CRYSTRAN, Poole,

United Kingdom) and air-dried at room temperature. IR spectra were collected using an FT-IR microscope (Thermo Scientific, Nicolet iN10) scanning from 4000 to 675 cm-1 with a spectral resolution of 4 cm-1 and an aperture size set at 30 X 30 µm. For each section, 10 spectra were acquired in 10 different muscle fibres. Each spectrum resulted from 64 accumulated scans. The accumulated spectra were averaged and subtracted from a background spectrum obtained at the start of the scan by accumulating 128 scans.

2.6. Infrared spectra pre-treatment

The spectra acquired were analysed using TQAnalyst software (V 9.5.0, Thermo Fisher Scientific Inc., Waltham, MA, USA). All spectra were first submitted to multiplicative signal correction (MSC) so that analytical artefacts would not be taken into account. The second derivative of the spectra was calculated, and a Savistky-Golay filter with 9 points and a third-degree polynomial was applied to improve the data resolution.

2.7. Statistical analysis

The analysis on the infrared spectra was focused on the 1600-1700 cm^{-1} region mostly assigned to the amide I band of proteins (Barth & Zscherp, 2002). Principal component analysis (PCA) was performed on all spectra to explore similarities between the samples without prior assumptions, using the absorbance at each measured wavenumber as a variable. Principal component representation was used to determine which variables had the most weight to describe the variability between the samples and the pressure conditions. Measurement of the peak heights at 1655 cm^{-1} and 1628 cm^{-1} was performed, and the resulting data were shifted to improve the graphical representation.

For histological data, statistical analysis was carried out using Statgraphics Centurion 18

182 software (Statgraphics Technologies, Inc., The Plains, VA, USA). Multivariate analysis of
183 variance (ANOVA) was performed on the data to determine significant differences between
184 the levels of pressure applied while taking intraspecies variability into account. Multiple
185 range tests were used to identify which means were significantly different according to
186 Fisher's least significant difference (LSD) test ($p < 0.05$).
187
188 The data in all the figures are expressed as the means ± standard error.
189

190 3. Results

191

192 3.1. Effect of HP on the microstructure of salmon muscle

193 Figure 1 shows representative histological images of the HES- and Picrosirius red stained
194 cross-sections.
195 HES staining (Figure 1A) allowed us to assess the effects of HP on salmon microstructure.
196 The HES-stained control fibres appeared tight, with narrow spaces between cells. At 200
197 MPa, the ECS increased compared to that of the control. Similar results were found on
198 cold-smoked Atlantic salmon treated with HP above 400 MPa for 30 and 60 s
199 (Gudbjornsdottir et al., 2010) and on raw salmon muscle processed at 300 MPa
200 (Gudmundsson & Hafsteinsson, 2001). Conversely, Chéret et al. (2005) observed the
201 opposite effect on sea bass (*Dicentrarchus labrax L.*) fillet, with a decrease in the ECS with
202 increasing pressure from 200 to 500 MPa, which they attributed to gelation of the
203 myofibrillar proteins.
204 After pressurization at 400 and 600 MPa, the appearance of the fibres changes and
205 becomes smoother with brighter red staining, which could be a consequence of an
206 increase in protein density and/or protein coagulation.
207 Image analysis with ImageJ software was used to precisely quantify the changes in

208 microstructure. Collagen, which appears in purple in Figure 1A, was calculated as part of
209 the ECS.
210 The high-pressure treatment resulted in shrinkage of the fibres (Figure 2A) and an
211 increase in the ECS (Figure 2B), suggesting that this increase was at least partly a
212 consequence of lateral shrinkage of the muscle fibres. Although significant differences in
213 fibre size were demonstrated between the 200 MPa and 400 MPa samples, overall, the
214 treated samples showed little cross-sectional area (CSA) variation among them. However,
215 the treatment at 600 MPa resulted in a large increase in ECS, even though the average
216 fibre size was not modified compared to that at 400 MPa. Similarly, Gudbjornsdottir et al.
217 (2010) observed a significant increase in the ECS for samples pressurized to 600 MPa or
218 more. However, the increase in ECS was related to the shrinkage of muscle fibres,
219 contrary to our results. Our results could be explained by a disruption of the connective
220 tissue, which no longer holds the fibres together, as suggested by Figure 1B.
221
222 **3.1.2 Picrosirius red staining**
223 The images of the picrosirius red-stained sections are shown in Figure 1B: the fibres are
224 coloured yellow, and the connective tissue is coloured red. For the HES-stained sections,
225 the control fibres appeared close to each other, with a thin layer of connective tissue
226 between the cells. The fibre colour also changes with increasing pressure, becoming more
227 orange. From 400 MPa, connective tissue appears thicker and brighter red.
228 Compared to HES staining, which was used to precisely evaluate the fibre characteristics,
229 picrosirius red staining allowed estimating the amount of space occupied distinctively by
230 the fibres, connective tissue and ECSs, as presented in Figure 3A, 3B and 3C,
231 respectively.
232
233 For the unpressurized samples, the fibres represent 57.7% (± 0.6%) of the total area, 3.1%

234 for the connective tissue and 3.0% for the ECS. Only the fibres that were fully inside the
235 optical area were taken into account for the calculation, which explains why the sum was
236 not equal to 100%.
237 The pressurization of the salmons at 200 MPa resulted in a marked increase in the area
238 occupied by the ECS and a slight decrease in the fibre area, whereas no significant effect
239 was observed for the connective tissue. At 400 MPa, no additional effect was observed on
240 the fibres and ECS, but the percentage of area occupied by the connective tissue was
241 doubled compared to that at 200 MPa, which we assumed could be explained by a
242 loosening of the collagen structure.
243 At 600 MPa, significant decreases in the fibres and the connective tissue area were
244 measured, correlated with a large increase in the ECS.
245

246 **3.2. Effects of high-pressure treatment on the secondary structure of salmon**
247 **proteins**

248 Mid-infrared spectroscopy is a powerful tool to characterize protein secondary structures
249 based on the principle that the vibrational frequencies of a molecule are affected by the
250 strength of its bonds and the mass of its vibrating atoms (Barth & Zscherp, 2002). In the
251 present study, vibrational spectra were acquired from approximately 120 myofibres for
252 each pressure condition.
253 PCA was performed on all the whole spectra (675-4000 cm^{-1}) and allowed identifying the
254 1700-1600 cm^{-1} band as the most discriminant for HP treatments.
255 This band is assigned to the amide I band of proteins and is more specifically related to
256 the vibration of the stretching of C=O bonds. It is strongly related to the secondary
257 structure of the proteins (Barth & Zscherp, 2002; Jackson & Mantsch, 1995).
258 Consequently, the data analysis focused on the 1700-1600 cm^{-1} part of the spectra
259 (Figures 4 - 5).

With increasing pressure, the second-derivative spectra (Figure 4) clearly show a decrease in absorbance at 1655 cm^{-1} assigned to α-helices (Barth, 2007; Jackson & Mantsch, 1995) and an increase in absorbance in the 1640-1620 cm^{-1} range. The band occurring at 1628 cm^{-1} is assigned to denatured aggregated β-sheet components (intermolecular), while the band between 1630 and 1640 cm^{-1} is assigned to antiparallel β-sheet structures (intramolecular) (Jackson and Mantsch, 1995; Bocker et al., 2006, Wu et al. 2007).

PCA (Figure 5) confirms that the dissimilarities between the pressure groups were strongly correlated to the first principal component, which was mainly explained by bands at 1655 cm^{-1} and 1628 cm^{-1} reflecting myofibre protein denaturation (Astruc et al. 2012).

Quantification of the peak heights at 1655 cm^{-1} and 1628 cm^{-1} was performed to study the evolution of the secondary structure with pressure (figure 6). Previous studies conducted on fish treated with HP (Larrea-Wachtendorff et al., 2015; Martínez et al., 2017) also focused on the amide I band of the FT-IR spectra and found a similar evolution of the secondary structure, i.e., a decrease in the α-helix content and an increase in the content of aggregated β-sheet structures. Villamonte et al. (2015) focused on the effects of HP on sarcoplasmic proteins extracted from hake and observed the same evolution of secondary structure correlated to a decrease of their emulsifying properties. The changes of the sarcoplasmic proteins structure also caused their aggregation, which can result in an increase of the hardness of the fish meat. The decrease of α-helix and increase of aggregated β-sheet structures was also measured by Cando et al. (2014) on myofibrillar proteins isolated from hake and treated by HP. The pressure treatment induced the formation of gels which were less rigid and softer than gels formed by thermal denaturation of the proteins. The authors suggested that the increase of aggregated β-sheet structures

286 could be the consequence of a gelling process.
287 Pressure denaturation of muscle proteins resulted in similar modifications of their
288 secondary structure than after thermal treatment (Astruc et al., 2012; Ovissipour et al.,
289 2017). However, in the present study, the denaturation cannot be caused by temperature
290 as it did not exceed 33.6°C. Protein denaturation occurs during HP due to destabilisation
291 of non-covalent interactions in the tertiary and secondary structures, particularly
292 hydrophobic and ionic interactions because their disruption is associated with a negative
293 change of volume and thus a compaction of the molecule (Chapleau et al., 2004;
294 Heremans, 1982; Mozhaev et al., 1994). High pressure acts by altering the balance of
295 intermolecular and solvent–protein interactions. Contrary to thermal denaturation, HP
296 treatments do not lead to the formation of intermolecular hydrogen bonds (Chapleau et al.
297 2004).
298

299 ## 4. Discussion

300

301 The results of the histological analysis show that HP causes a decrease in the fibre size
302 regardless of the level of pressure applied, which is likely to be responsible for the ECS
303 increase. The shrinkage of the fibres could be related to water flows between the muscle
304 cells and the ECS. Several authors have shown a decrease in the water holding capacity
305 of fish submitted to HP, which supports this hypothesis (Chéret et al., 2005; Jiranuntakul et
306 al., 2018; Lakshmanan et al., 2007; Ramirez-Suarez & Morrissey, 2006). Chéret et al.
307 (2005) additionally studied the exudation of sea bass fillets after pressurization but did not
308 observe any modification caused by HP.
309 Furthermore, we have shown that pressure above 400 MPa resulted in a change in
310 connective tissue appearance and size. This alteration could be due to a change in the
311 collagen structure. Collagen is formed of a triple helix mainly stabilized by hydrogen and

312 covalent bonds connecting hydroxyproline from one strand to amide carboxyl from another
313 strand (Benjakul et al., 2012) and should therefore be relatively resistant to HP (Truong et
314 al., 2015). However, Kaur et al. (2016) studied the effects of HP on the structure of bovine
315 meat and suggested that pressure, by disrupting the non-covalent bonds, could disturb the
316 molecule stability. Fish collagen contains smaller amounts of proline and hydroxyproline
317 and is therefore less stable than mammalian collagen which supports our hypothesis
318 (Benjakul et al., 2012).
319 Kaur et al. (2016) also observed a decrease in connective tissue on raw pork treated by
320 HP (600 MPa, 10 min), which they attributed to a possible rise in temperature during high-
321 pressure processing associated with a decrease in denaturation temperature of the
322 collagen caused by the destabilization of non-covalent bonds. During the processing of our
323 samples, we measured a rise in temperature from 20°C to 29.4°C and 33.6°C for the 400
324 MPa and 600 MPa treatments, respectively. The denaturation of fish collagen was reported
325 to occur at between 30°C and 40°C (Benjakul et al., 2012; Hastings et al., 1985), and the
326 slight increase in temperature might have participated in the loosening of the connective
327 tissue at 400 MPa and the partial denaturation at 600 MPa caused by the high-pressure
328 treatment.
329 It is worth noting that after pressurization at 600 MPa, the ECS size is substantially
330 increased even though the fibre cross-sectional area is not significantly modified. It is
331 unlikely that the overall volume of the samples was expanded by the treatment because
332 pressure rather favours molecular states which are related with a decreased volume
333 (Mozhaev et al., 1994). However, this phenomenon was correlated with the decrease of
334 the connective tissue area at 600 MPa compared to 400 MPa, and it is therefore likely that
335 the pressure induced denaturation of collagen caused a partial disruption of the connective
336 tissue which could no longer hold the fibres together, explaining the increase of the ECS.
337 This could have possibly happened after depressurization, during the preparation of the

samples.

All levels of HP resulted in a modification of the salmon muscle secondary structure. After pressurization at 200 MPa, myofibres contained a smaller amount of α-helices and more aggregated β-sheet structures, associated with the compaction of the fibres and larger ECS than that of the control. This modification of the secondary structure was enhanced at higher levels of pressure. After pressurization at 400 MPa, connective tissue integrity was altered and therefore occupied an increased surface are compared to that of the control and 200 MPa samples. When pressurization at 600 MPa was applied, connective tissue was found to be partially degraded, leading to an expansion of the ECS.

Myofibrillar proteins are the most abundant proteins in muscle cells, with 50-60% myosin (Venugopal & Shahidi, 1996) and are mainly organized in α-helices (Wang et al., 2021; Xu et al., 2020). Several authors (Angsupanich & Ledward, 1998; Arnaud et al., 2018; Larrea-Wachtendorff et al., 2015) have studied the thermal denaturation of proteins from fishes previously treated by HP, and all found that myofibrillar proteins were denatured by pressures above 200 MPa, with denaturation enthalpies decreasing all the more that pressure was increased. The protein secondary structure is stabilized by hydrogen bonds, which are known to be resistant or even strengthened by HP (Mozhaev et al., 1994; Oliveira et al., 2017) because of the negative volume changes that are associated with the formation of these bonds. Boonyaratanakornkit et al. (2002) reported that these bonds were, however, modified by HP, with a reduced length and a possible promotion of intermolecular hydrogen bonds to the detriment of intramolecular hydrogen bonds. HP, by unfolding myofibrillar proteins and changing the properties of the hydrogen bonds, could therefore result in the destabilization of part of the α-helixes and an increase in the content of β-sheets. The consequent compression of myofibrillar proteins might explain the observed decrease in myofibre size.

These alterations in muscle structure are linked to pressure-induced modifications of fish sensory properties. Authors have reported significant changes in salmon colour after pressurization, especially increased lightness (Gudbjornsdottir et al., 2010; Yagiz et al., 2009). Although the mechanisms responsible for this discoloration are still unclear, evidence shows that it could be due to the denaturation or coagulation of myofibrillar proteins. The unfolding of these proteins could indeed modify their surface properties and affect the way they absorb and reflect light (Kruk et al., 2011; Suemitsu & Cristianini, 2019). The decrease in α-helical structures that we observed as well as the histological analysis, which show that the myofibre cross-sections become smoother with pressure, support the hypothesis that the change in colour caused by HP is linked to the denaturation of muscle proteins rather than the alteration of carotenoid pigments. These molecules are responsible for the distinctive orange colour of salmon and are likely unaltered by mechanical treatments such as HP (Martínez-Delgado et al., 2017).

In most cases, high-pressure treatments increase the hardness of fish muscles (Oliveira et al., 2017), and this change in texture has been associated with a higher compaction of the fibres after treatment and a preservation of collagen by pressure (Truong et al., 2015). In contrast, we observed an increase in the intercellular space and an alteration in connective tissue integrity in this study. Arnaud et al. (2018) suggested that the increased hardness observed on salmon after pressurization at 300 MPa could be a result of protein aggregation, which is consistent with the increase in the β-sheet structure that we measured.

In the present study, FT-IR spectral analysis could not be performed on the connective tissue because the spatial resolution of a laboratory FT-IR microspectrometer is too low (best acquisition area of 10 µm x 10 µm) to precisely target the endomysium. Further analyses using a synchrotron infrared beamline (Astruc et al., 2012) or Raman microspectroscopy technique will allow us to achieve a sufficient spatial resolution (3x3 µm

for synchrotron-FTIR microspectroscopy; 1 x 1 µm for Raman microspectroscopy) to investigate the intramuscular connective tissue in order to better understand the modifications of the connective tissue affected by high-pressure treatment.

5. Conclusion

Most interpretations of the pressure-induced modifications of fish muscles are based on physical rules such as Le Chatelier's principle (Mozhaev et al., 1994) or on experimental data obtained from extracted proteins. However, these interpretations fail to take into consideration the high level of organization and complexity of the muscular structure. The combination of histological and FT-IR microspectroscopy analysis allowed us to investigate the microstructure and myofibre protein macromolecular structure *in situ* and concomitantly. Supplementary analysis of quality parameters of Atlantic salmon treated by HP, such as colour, texture and water holding capacity, would provide helpful data to explain the relations between the microstructure and the technological properties of salmon meat.

Acknowledgments

This study was funded by Pays de la Loire as part of the PATACHON project. The authors would like to thank Anthony Ogé for carrying out the high-pressure treatments and Eloïse Ribette-Lancelot for the help to analyse the spectral data.

Conflicts of interest

The authors declare that they have no known competing financial interests or personal relationships that could have appeared to influence the work reported in this paper.

References

Angsupanich, K., & Ledward, D. A. (1998). High pressure treatment effects on cod (Gadus morhua) muscle. *Food Chemistry*, *63*(1), 39–50. https://doi.org/10.1016/S0308-8146(97)00234-3

Arnaud, C., Lamballerie, M. de, & Pottier, L. (2018). Effect of high pressure processing on the preservation of frozen and re-thawed sliced cod (Gadus morhua) and salmon (Salmo salar) fillets. *High Pressure Research*, *38*(1), 62–79. https://doi.org/10.1080/08957959.2017.1399372

Astruc, T., Peyrin, F., Vénien, A., Labas, R., Abrantes, M., Dumas, P., & Jamme, F. (2012). In situ thermal denaturation of myofibre sub-type proteins studied by immunohistofluorescence and synchrotron radiation FT-IR microspectroscopy. *Food Chemistry*, *134*(2), 1044–1051. https://doi.org/10.1016/j.foodchem.2012.03.012

Aubourg, S. P. (2018). Impact of high-pressure processing on chemical constituents and nutritional properties in aquatic foods: A review. *International Journal of Food Science & Technology*, *53*(4), 873–891. https://doi.org/10.1111/ijfs.13693

Aubourg, S. P., Rodríguez, A., Sierra, Y., Tabilo-Munizaga, G., & Pérez-Won, M. (2013). Sensory and Physical Changes in Chilled Farmed Coho Salmon (Oncorhynchus kisutch): Effect of Previous Optimized Hydrostatic High-Pressure Conditions. *Food and Bioprocess Technology*, *6*(6), 1539–1549. https://doi.org/10.1007/s11947-012-0799-4

Barth, A., & Zscherp, C. (2002). What vibrations tell about proteins. *Quarterly Reviews of Biophysics*, *35*(4), 369–430. https://doi.org/10.1017/S0033583502003815

Benjakul, S., Nalinanon, S., & Shahidi, F. (2012). Fish Collagen. In *Food Biochemistry and*

Food Processing: Second Edition (pp. 365–387). https://doi.org/10.1002/9781118308035.ch20

Boonyaratanakornkit, B. B., Park, C. B., & Clark, D. S. (2002). Pressure effects on intra- and intermolecular interactions within proteins. *Biochimica et Biophysica Acta (BBA) - Protein Structure and Molecular Enzymology*, *1595*(1), 235–249. https://doi.org/10.1016/S0167-4838(01)00347-8

Cando, D., Moreno, H. M., Tovar, C. A., Herranz, B., & Borderias, A. J. (2014). Effect of High Pressure and/or Temperature over Gelation of Isolated Hake Myofibrils. Food and Bioprocess Technology, 7(11), 3197–3207. https://doi.org/10.1007/s11947-014-1279-9

Chapleau, N., Mangavel, C., Compoint, J.-P., & Lamballerie-Anton, M. de. (2004). Effect of high-pressure processing on myofibrillar protein structure. Journal of the Science of Food and Agriculture, 84(1), 66–74. https://doi.org/10.1002/jsfa.1613

Chéret, R., Chapleau, N., Delbarre-Ladrat, C., Verrez-Bagnis, V., & Lamballerie, M. de. (2005). Effects of High Pressure on Texture and Microstructure of Sea Bass (Dicentrarchus labrax L.) Fillets. *Journal of Food Science*, *70*(8), e477–e483. https://doi.org/10.1111/j.1365-2621.2005.tb11518.x

de Alba, M., Pérez-Andrés, J. M., Harrison, S. M., Brunton, N. P., Burgess, C. M., & Tiwari, B. K. (2019). High pressure processing on microbial inactivation, quality parameters and nutritional quality indices of mackerel fillets. *Innovative Food Science & Emerging Technologies*, *55*, 80–87. https://doi.org/10.1016/j.ifset.2019.05.010

Directorate-General for Maritime Affairs and Fisheries (European Commission). (2020). The EU fish market: 2020 edition. Publications Office of the European Union. https://data.europa.eu/doi/10.2771/664425

461 Fogarty, C., Whyte, P., Brunton, N., Lyng, J., Smyth, C., Fagan, J., & Bolton, D. (2019).
462 Spoilage indicator bacteria in farmed Atlantic salmon (Salmo salar) stored on ice for 10
463 days. *Food Microbiology*, *77*, 38–42. https://doi.org/10.1016/j.fm.2018.08.001

464 Gudbjornsdottir, B., Jonsson, A., Hafsteinsson, H., & Heinz, V. (2010). Effect of high-
465 pressure processing on Listeria spp. And on the textural and microstructural properties of
466 cold smoked salmon. *LWT - Food Science and Technology*, *43*(2), 366–374.
467 https://doi.org/10.1016/j.lwt.2009.08.015

468 Gudmundsson, M., & Hafsteinsson, H. (2001). Effect of electric field pulses on
469 microstructure of muscle foods and roes. *Trends in Food Science & Technology*, *12*(3),
470 122–128. https://doi.org/10.1016/S0924-2244(01)00068-1

471 Hastings, R. J., Rodger, G. W., Park, R., Matthews, A. D., & Anderson, E. M. (1985).
472 Differential Scanning Calorimetry of Fish Muscle: The Effect of Processing and Species
473 Variation. *Journal of Food Science*, *50*(2), 503–506. https://doi.org/10.1111/j.1365-
474 2621.1985.tb13437.x

475 Heremans, K. (1982). High pressure effects on proteins and other biomolecules. Annual
476 Review of Biophysics and Bioengineering, 11, 1–21.
477 https://doi.org/10.1146/annurev.bb.11.060182.000245

478 Jackson, M., & Mantsch, H. H. (1995). The Use and Misuse of FTIR Spectroscopy in the
479 Determination of Protein Structure. *Critical Reviews in Biochemistry and Molecular*
480 *Biology*, *30*(2), 95–120. https://doi.org/10.3109/10409239509085140

481 Jiranuntakul, W., Nakwiang, N., Berends, P., Kasemsuwan, T., Saetung, T., & Devahastin,
482 S. (2018). Physicochemical, Microstructural, and Microbiological Properties of Skipjack
483 Tuna (Katsuwonus pelamis) After High-Pressure Processing. *Journal of Food Science*,

83(9), 2324–2336. https://doi.org/10.1111/1750-3841.14318

Kaur, L., Astruc, T., Vénien, A., Loison, O., Cui, J., Irastorza, M., & Boland, M. (2016). High pressure processing of meat: Effects on ultrastructure and protein digestibility. *Food & Function*, *7*(5), 2389–2397. https://doi.org/10.1039/c5fo01496d

Knorr, D., Heinz, V., & Buckow, R. (2006). High pressure application for food biopolymers. *Biochimica et Biophysica Acta (BBA) - Proteins and Proteomics*, *1764*(3), 619–631. https://doi.org/10.1016/j.bbapap.2006.01.017

Kruk, Z. A., Yun, H., Rutley, D. L., Lee, E. J., Kim, Y. J., & Jo, C. (2011). The effect of high pressure on microbial population, meat quality and sensory characteristics of chicken breast fillet. *Food Control*, *22*(1), 6–12. https://doi.org/10.1016/j.foodcont.2010.06.003

Lakshmanan, R., Parkinson, J. A., & Piggott, J. R. (2007). High-pressure processing and water-holding capacity of fresh and cold-smoked salmon (Salmo salar). *LWT - Food Science and Technology*, *40*(3), 544–551. https://doi.org/10.1016/j.lwt.2005.12.003

Larrea-Wachtendorff, D., Tabilo-Munizaga, G., Moreno-Osorio, L., Villalobos-Carvajal, R., & Pérez-Won, M. (2015). Protein Changes Caused by High Hydrostatic Pressure (HHP): A Study Using Differential Scanning Calorimetry (DSC) and Fourier Transform Infrared (FTIR) Spectroscopy. *Food Engineering Reviews*, *7*(2), 222–230. https://doi.org/10.1007/s12393-015-9107-1

Martínez, M. A., Velazquez, G., Cando, D., Núñez-Flores, R., Borderías, A. J., & Moreno, H. M. (2017). Effects of high pressure processing on protein fractions of blue crab (Callinectes sapidus) meat. *Innovative Food Science & Emerging Technologies*, *41*, 323–329. https://doi.org/10.1016/j.ifset.2017.04.010

Martínez-Delgado, A. A., Khandual, S., & Villanueva–Rodríguez, S. J. (2017). Chemical

stability of astaxanthin integrated into a food matrix: Effects of food processing and methods for preservation. *Food Chemistry*, *225*, 23–30. https://doi.org/10.1016/j.foodchem.2016.11.092

Mozhaev, V. V., Heremans, K., Frank, J., Masson, P., & Balny, C. (1994). Exploiting the effects of high hydrostatic pressure in biotechnological applications. *Trends in Biotechnology*, *12*(12), 493–501. https://doi.org/10.1016/0167-7799(94)90057-4

Oliveira, F. A. de, Neto, O. C., Santos, L. M. R. dos, Ferreira, E. H. R., & Rosenthal, A. (2017). Effect of high pressure on fish meat quality – A review. *Trends in Food Science & Technology*, *66*, 1–19. https://doi.org/10.1016/j.tifs.2017.04.014

Ovissipour, M., Rasco, B., Tang, J., & Sablani, S. (2017). Kinetics of Protein Degradation and Physical Changes in Thermally Processed Atlantic Salmon (Salmo salar). *Food and Bioprocess Technology*, *10*(10), 1865–1882. https://doi.org/10.1007/s11947-017-1958-4

Park, D.-H., Jung, J.-G., Jung, B.-R., Kim, G., Lee, H., Kim, H.-A., & Bang, M.-A. (2015). Changes in Salmon (Oncorhynchus keta) Flesh Quality Following Ultra-High Pressure Treatment and 30 d of Chilled Storage. *Journal of Food Science*, *80*(1), M142–M146. https://doi.org/10.1111/1750-3841.12714

Ramirez-Suarez, J. C., & Morrissey, M. T. (2006). High Hydrostatic Pressure and Heat Treatment Effects on Physicochemical Characteristics of Albacore Tuna (Thunnus alalunga) Minced Muscle. *Journal of Aquatic Food Product Technology*, *15*(1), 5–17. https://doi.org/10.1300/J030v15n01_02

Suemitsu, L., & Cristianini, M. (2019). Effects of high pressure processing (HPP) on quality attributes of tilapia (Oreochromis niloticus) fillets during refrigerated storage. *LWT*, *101*, 92–99. https://doi.org/10.1016/j.lwt.2018.11.028

530 Truong, B. Q., Buckow, R., Nguyen, M. H., & Furst, J. (2017). Gelation of barramundi
531 (Lates calcarifer) minced muscle as affected by pressure and thermal treatments at low
532 salt concentration. Journal of the Science of Food and Agriculture, 97(11), 3781–3789.
533 https://doi.org/10.1002/jsfa.8242
534
535 Truong, B. Q., Buckow, R., Stathopoulos, C. E., & Nguyen, M. H. (2015). Advances in
536 High-Pressure Processing of Fish Muscles. *Food Engineering Reviews*, *7*(2), 109–129.
537 https://doi.org/10.1007/s12393-014-9084-9

538 Uresti, R. M., Velazquez, G., Ramírez, J. A., Vázquez, M., & Torres, J. A. (2004). Effect of
539 high-pressure treatments on mechanical and functional properties of restructured products
540 from arrowtooth flounder (Atheresthes stomias). Journal of the Science of Food and
541 Agriculture, 84(13), 1741–1749. https://doi.org/10.1002/jsfa.1876

542 Venugopal, V., & Shahidi, F. (1996). Structure and composition of fish muscle. Food
543 Reviews International, 12(2), 175–197. https://doi.org/10.1080/87559129609541074

544 Wang, Y.-Y., Tayyab Rashid, M., Yan, J.-K., & Ma, H. (2021). Effect of multi-frequency
545 ultrasound thawing on the structure and rheological properties of myofibrillar proteins from
546 small yellow croaker. *Ultrasonics Sonochemistry*, *70*, 105352.
547 https://doi.org/10.1016/j.ultsonch.2020.105352

548 Xu, Y., Wang, R., Zhao, H., Yin, Y., Li, X., Yi, S., & Li, J. (2020). Effect of heat treatment
549 duration on the interaction between fish myosin and selected flavor compounds. *Journal of*
550 *the Science of Food and Agriculture*, *100*(12), 4457–4463.
551 https://doi.org/10.1002/jsfa.10486

552 Yagiz, Y., Kristinsson, H. G., Balaban, M. O., Welt, B. A., Ralat, M., & Marshall, M. R.
553 (2009). Effect of high pressure processing and cooking treatment on the quality of Atlantic

554 salmon. *Food Chemistry*, *116*(4), 828–835.
555 https://doi.org/10.1016/j.foodchem.2009.03.029

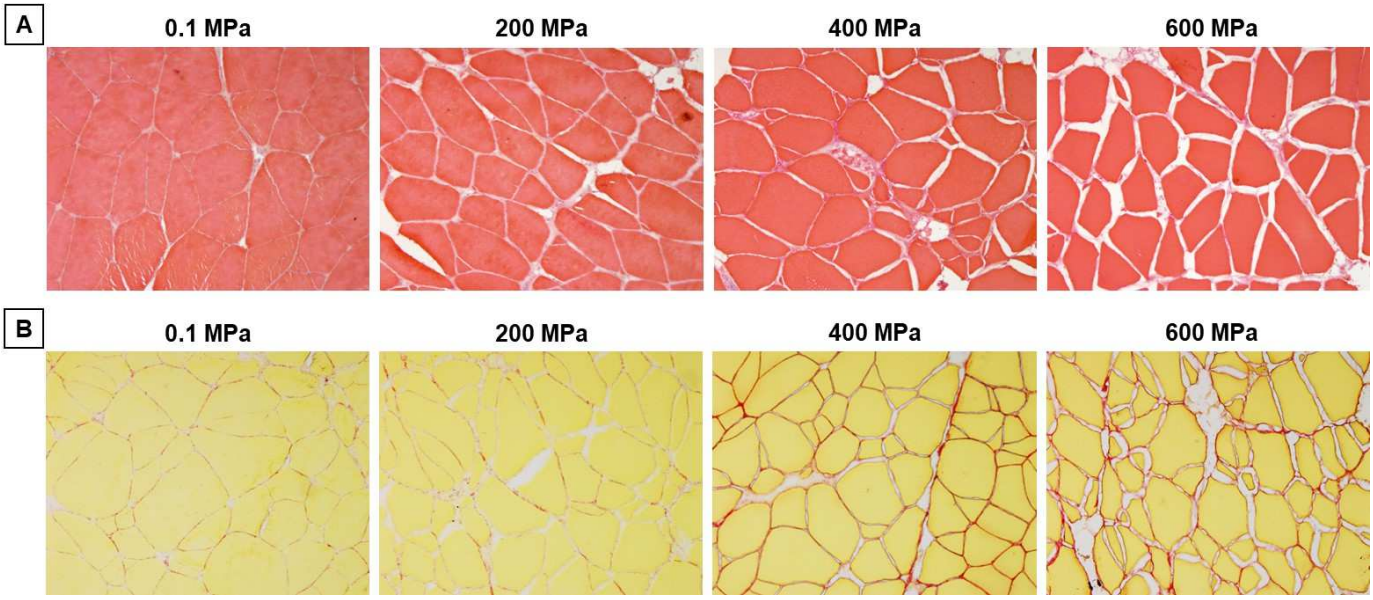

Figure 1: Histological sections of non-pressurized (0.1 MPa) and pressurized (200, 400 and 600 MPa, 5 min) salmon muscle. HES staining (A) colours the fibres red. Picrosirius red staining (B) colours the fibres yellow and the connective tissue red. Scale: 50 mm = 100 µm

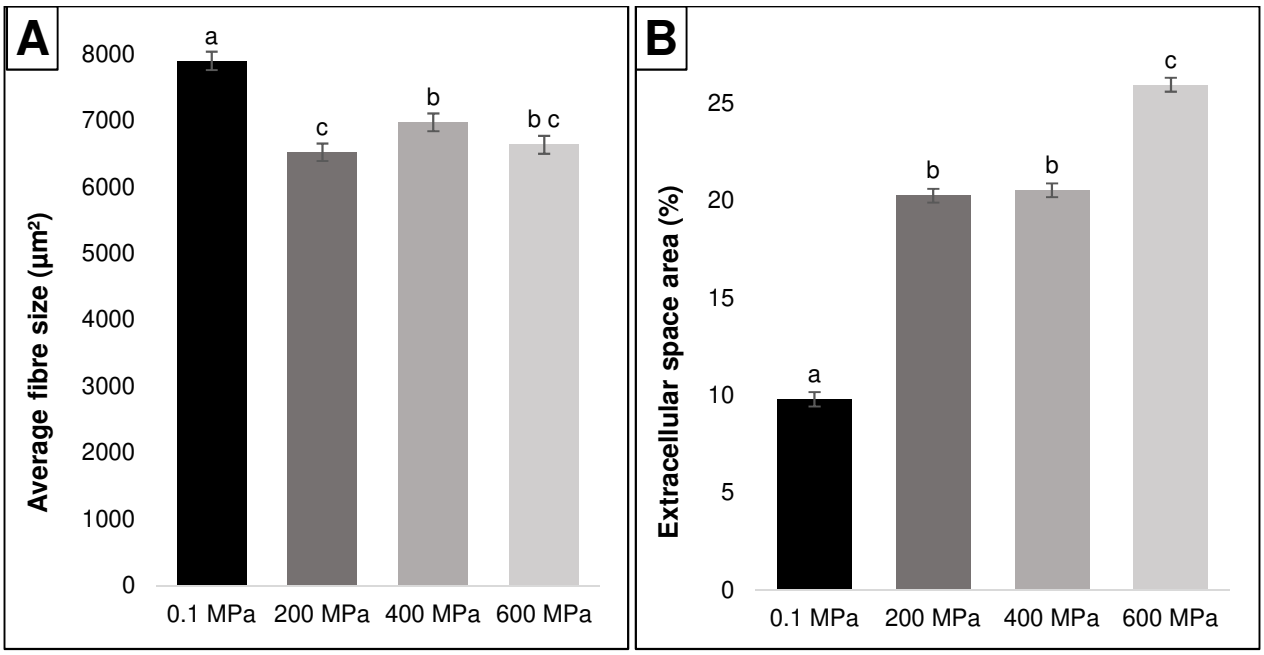

Figure 2: Average fibre size in µm² (A) and area from extracellular space in % (B) for non-pressurized (0.1 MPa) and pressurized (200, 400 and 600 MPa, 5 min) salmon (n=12) measured on HES-stained sections. The results are expressed as the mean ± standard error. Means with different letters are significantly different ($p < 0.05$).

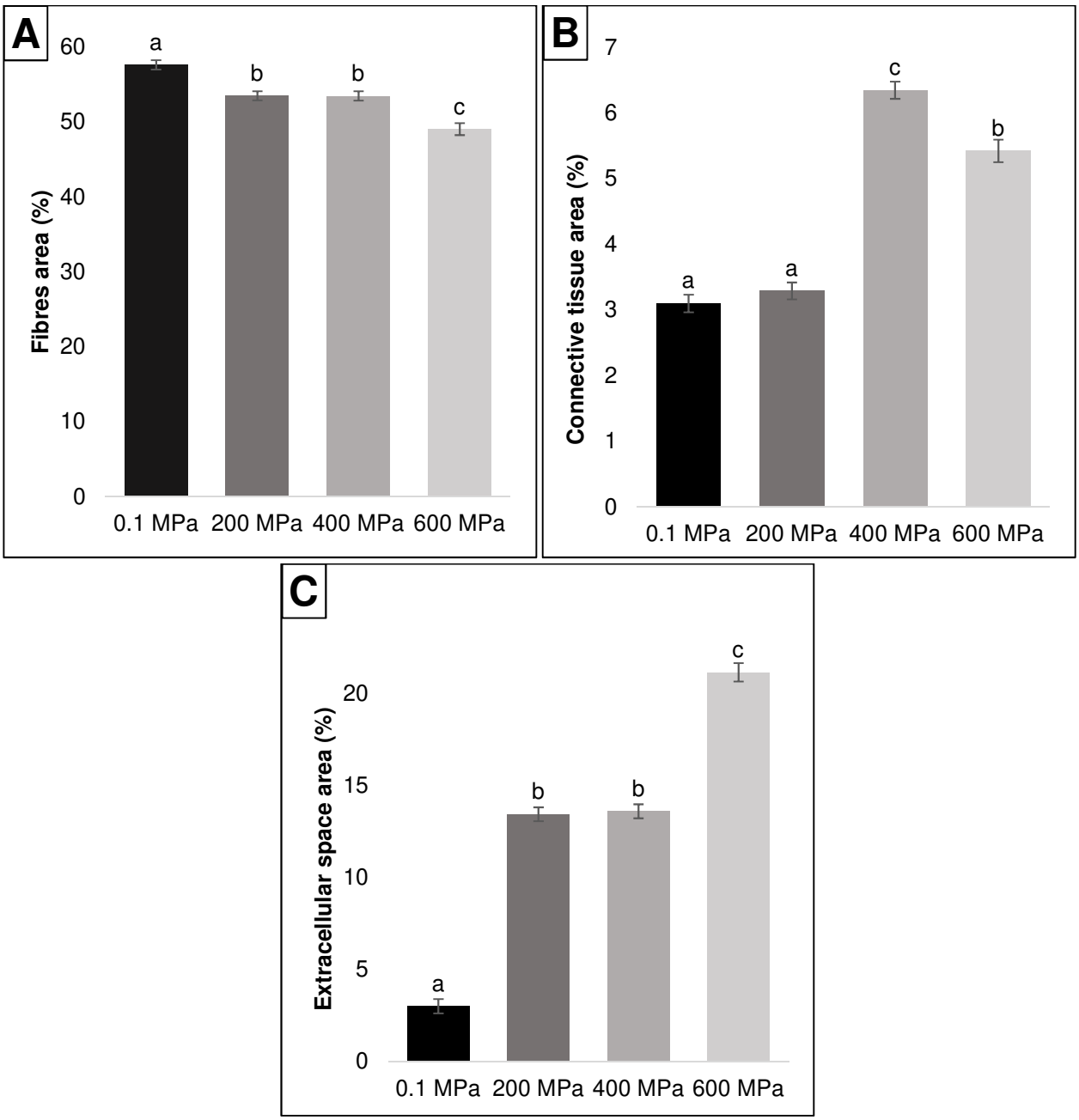

Figure 3: Percentage of the total section area from fibres (A), connective tissue (B) and extracellular space (C) for non-pressurized (0.1 MPa) and pressurized (200, 400 and 600 MPa, 5 min) salmon (n=12) measured on Picrosirius red-stained sections. The results are expressed as the mean ± standard error. Means with different letters are significantly different ($p < 0.05$).

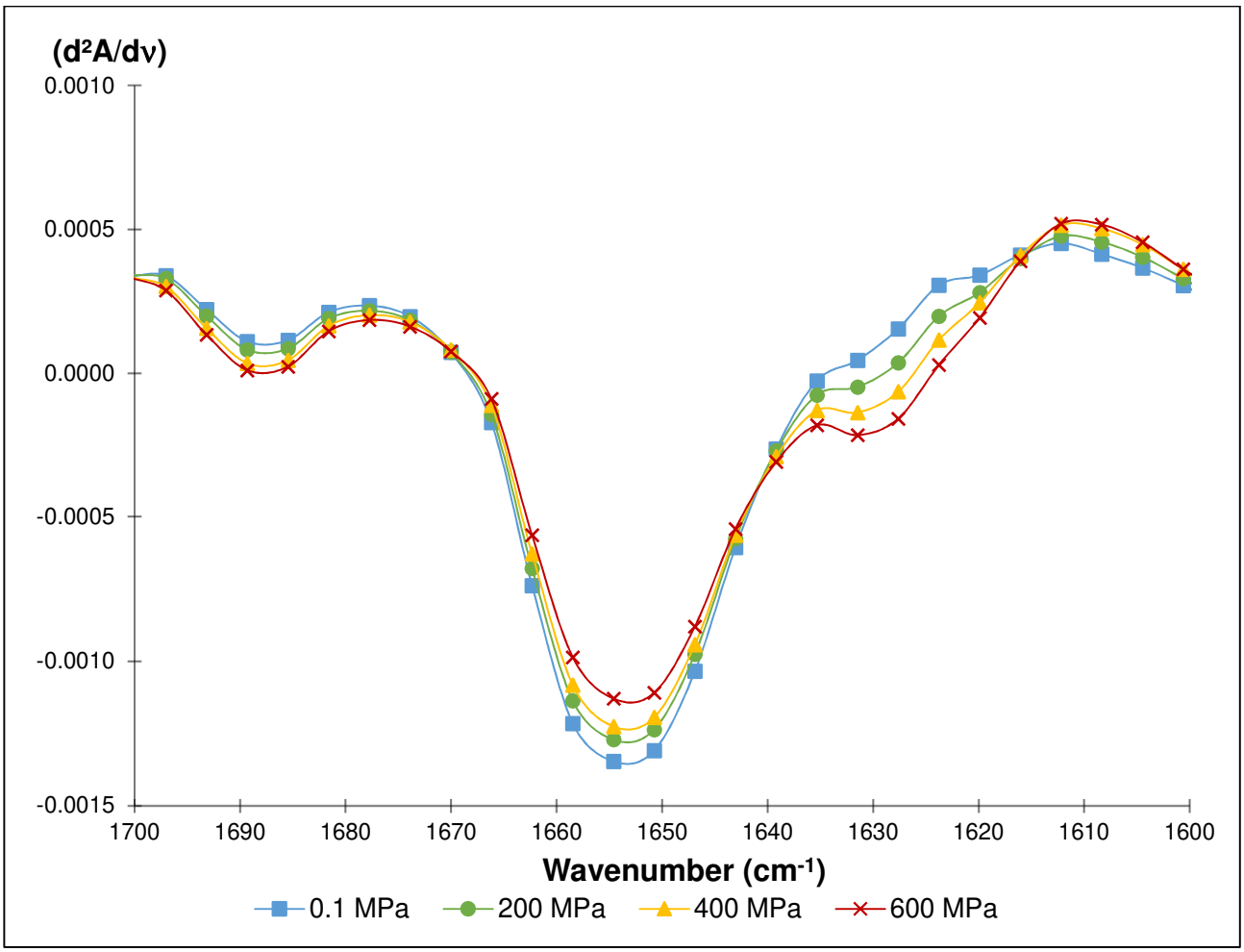

Figure 4: Second-derivative mean infrared spectra (1700-1600 cm^{-1}) obtained in muscle fibres of non-pressurized (0.1 MPa) and pressurized (200, 400 and 600 MPa, 5 min) salmons (n=12), each from approximately 120 spectra.

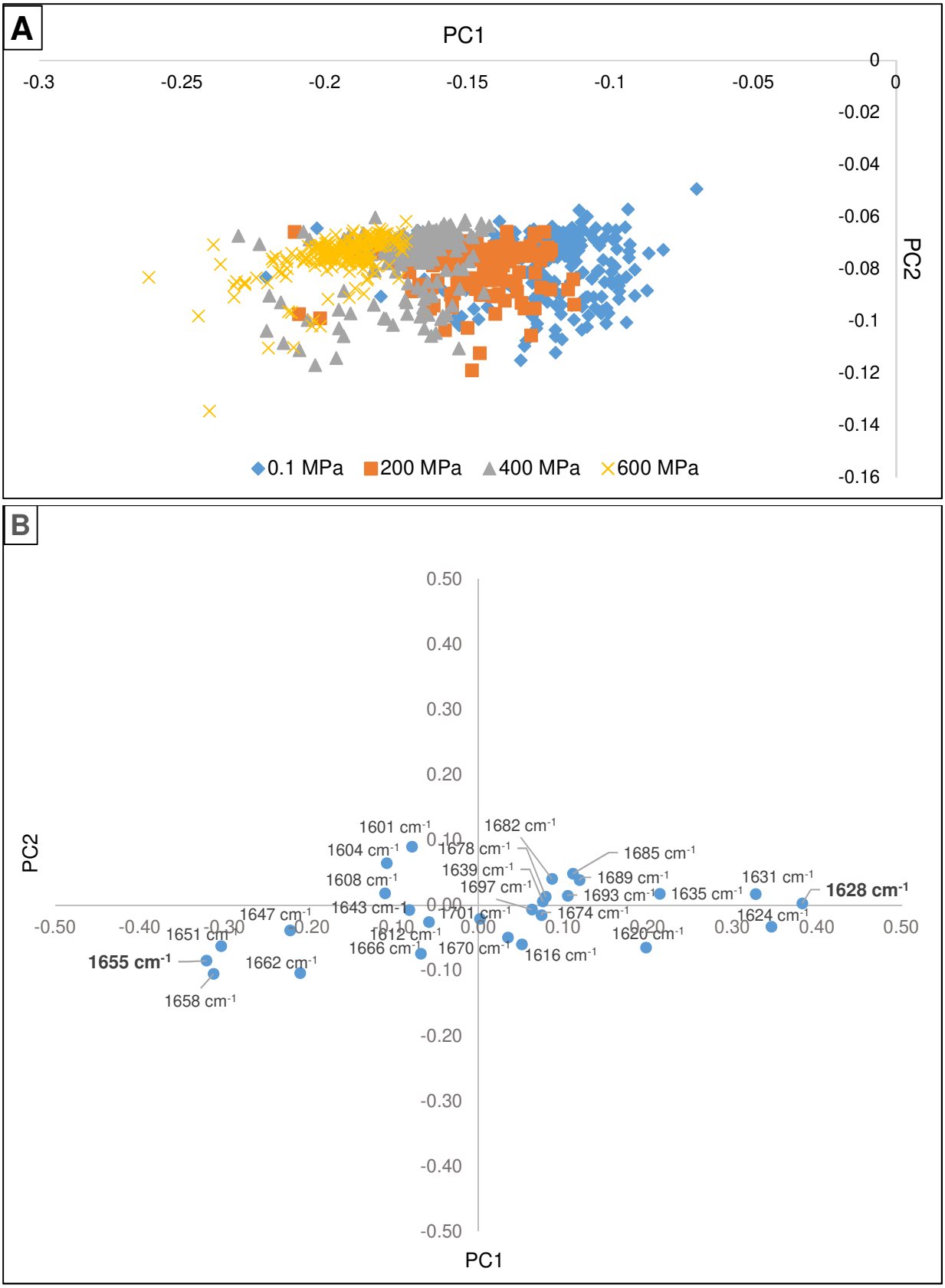

Figure 5: Principal component analysis (PCA) of the second derivative of the amide I (1600-1700 cm^{-1}) band (A). Pressure groups are separated along the first principal component (PC1).

The principal component graph (B) describes what wavenumbers contribute the most in describing each principal component. PC1 is mainly described by two bands with maximums at 1628 cm^{-1} and 1655 cm^{-1} and describes 56.77% of the variability between all samples.

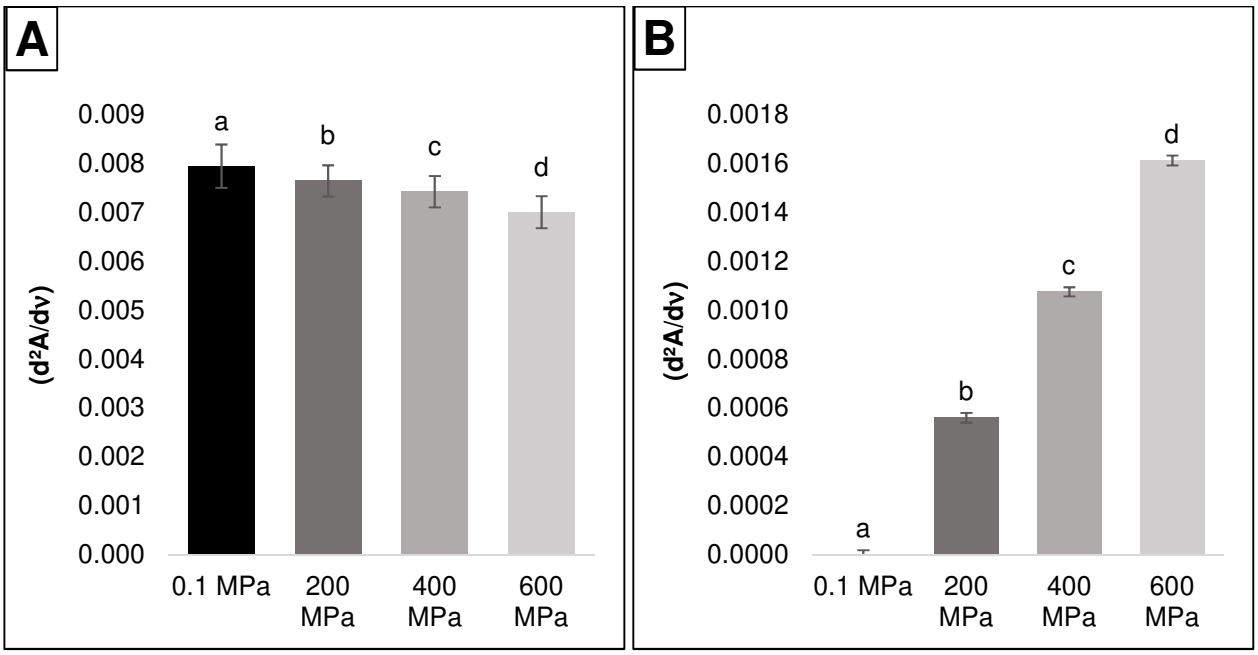

Figure 6: Evolution of α-helixes (A) and aggregated β-sheets (B) in salmon (n=12) muscle fibres measured by the height of the second-derivative spectra peaks at 1655 cm^{-1} and 1628 cm^{-1}, respectively. The results are expressed as the mean ± standard error. Means with different letters are significantly different ($p < 0.05$).

Effects of high-pressure treatment on the muscle structure of salmon (*Salmo salar*)

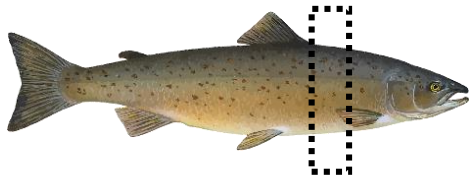

n = 12 salmons

High-pressure processing

Control, 200 MPa, 400 MPa, 600 MPa
5 min, 20°C

Histochemical analysis

- average fibre size
- amount of space occupied by :
  - the extracellular spaces (ECS)
  - the connective tissue

Infrared spectromicroscopy

- Infrared spectra acquired in the muscle fibres
- Evaluation of α-helix and aggregated β-sheet content

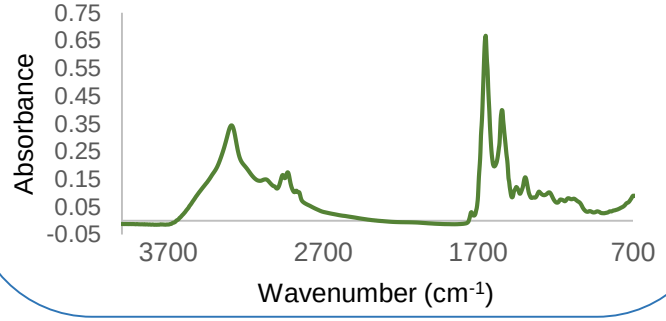

Results

- Shrinkage of the fibres from 200 MPa
- Increase of the ECS from 200 MPa
- Modification of the connective tissue at 400 MPa

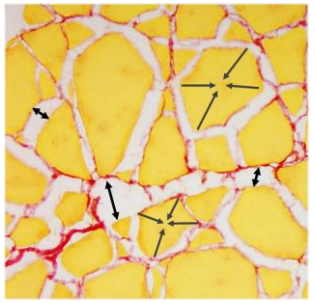

- Decrease of the α-helix and increase of the aggregated β-sheet with pressure